Prepared for submission to JHEP

NIKHEF 2021-027
BONN-TH-2021-10
ZU-TH 51/21
IPPP/21/40
CERN-TH-2021-158

Transverse momentum distributions in low-mass Drell-Yan lepton pair production at NNLO QCD

R. Gauld,[a,b] **A. Gehrmann–De Ridder,**[c,d] **T. Gehrmann,**[d] **E. W. N. Glover,**[e,f] **A. Huss,**[g] **I. Majer,**[c] **A. Rodriguez Garcia**[c]

[a] *Nikhef Theory Group, Science Park 105, 1098 XG Amsterdam, The Netherlands*
[b] *Bethe Center for Theoretical Physics & Physikalisches Institut der Universität Bonn*
[c] *Institute for Theoretical Physics, ETH, CH-8093 Zürich, Switzerland*
[d] *Department of Physics, University of Zürich, CH-8057 Zürich, Switzerland*
[e] *Institute for Particle Physics Phenomenology, Durham University, Durham DH1 3LE, UK*
[f] *Department of Physics, Durham University, Durham DH1 3LE, UK*
[g] *Theoretical Physics Department, CERN, CH-1211 Geneva 23, Switzerland*

E-mail: rgauld@uni-bonn.de, gehra@phys.ethz.ch, thomas.gehrmann@uzh.ch, e.w.n.glover@durham.ac.uk, alexander.huss@cern.ch, majeri@phys.ethz.ch, adrianro@phys.ethz.ch

Abstract: The production of lepton pairs at low invariant mass and finite transverse momentum resolves QCD dynamics at the boundary between the perturbative and non-perturbative domains. We investigate the impact of NNLO QCD corrections on these observables at energies corresponding to the BNL RHIC collider and to fixed-target experiments. Satisfactory perturbative convergence is observed in both cases. Only the collider data are found to be well-described by perturbative QCD, thus indicating the importance of non-perturbative effects in lepton-pair transverse momentum distributions at fixed target energies.

Contents

1 Introduction

The production of lepton pairs in hadronic collisions (Drell-Yan process, [1]) is mediated through a neutral electroweak gauge boson (γ^*, Z). It is a Standard Model benchmark process, which has been measured to very high precision at hadron colliders, thereby providing important insights into the structure of the colliding hadrons and into the dynamics of QCD through inclusive measurements or transverse momentum distributions. Collider measurements of the Drell-Yan process focus mainly on lepton pairs with high pair invariant mass Q, including in particular the Z resonance peak. The large mass scale Q ensures that a reliable theory description of the Drell-Yan cross section and of associated transverse momentum distributions can be obtained within perturbative QCD using fixed-order predictions, combined with transverse momentum resummation if required.

The phenomenological importance of the Drell-Yan process has been driving precision calculations in particle theory, which are by now accomplished to next-to-next-to-leading order (NNLO) for the fully differential Drell-Yan process [2,3]. Most recently, first results on the third order (N^{3}LO) corrections to the total Drell-Yan cross section [4] and its rapidity distribution [5] were derived. The Born-level kinematics (order α_s^0 in the QCD coupling constant) of the Drell-Yan process correspond to vanishing total transverse momentum p_T of the lepton pair. Consequently, the Drell-Yan transverse momentum distribution receives its leading-order (LO) contribution at order α_s^1. It is known to NNLO [6–8], which combines with transverse momentum resummation that has been derived [9–13] to the third logarithmic order (N^{3}LL).

At lepton pair invariant masses well below the Z resonance, virtual photon exchange largely dominates. With decreasing mass scale Q, the QCD coupling α_s increases, and the convergence of the perturbative expansion deteriorates. Low-mass Drell-Yan production can therefore probe the transition region between perturbative and non-perturbative QCD, and resolve aspects of the proton structure that go beyond the framework of collinear factorisation and parton distribution functions. Transverse momentum distributions of low-mass Drell-Yan pairs are particularly interesting in this context, since the simultaneous dependence on both Q and p_T enables to resolve the underlying dynamics in a multi-differential manner [14]. Low-mass Drell-Yan production at moderate and low transverse momenta is experimentally challenging at high-energy colliders like the LHC or the Tevatron, since the resulting leptons emerge with transverse momenta that are too low to be cleanly detected (the low pile-up conditions at LHCb may provide an exception). Data on low-mass Drell-Yan production are mainly from fixed-target experiments, as well as from RHIC at BNL.

Extensive studies of the available measurements on transverse momentum distributions in low-mass Drell-Yan production has been performed recently [15, 16], using next-to-leading order (NLO) QCD predictions [2, 17] as baseline for the theoretical predictions, combined with next-to-leading logarithmic resummation. It was found in [15, 16] that these perturbative NLO QCD predictions were insufficient to describe the majority of available data, thereby yielding evidence for the relevance of non-perturbative effects such as intrinsic partonic transverse momentum in the description of these observables. The low-mass Drell-Yan process has also been identified as ideal probe of transverse-momentum dependent parton distributions (TMDPDF), and first extractions of TMDPDFs for protons [18–20] and pions [21] have been performed on the available data sets.

This letter revisits the p_T distributions of low-mass Drell-Yan pairs in view of an improved perturbative description using for the first time NNLO QCD predictions. These are based on the calculation of NNLO QCD corrections to Z-boson production at large transverse momenta [7], which has been adapted to this kinematical situation. The calculation is implemented in the parton-level event generator NNLOJET, which uses the antenna subtraction method [22–24] to handle infrared singular real radiation at NNLO.

For the numerical evaluations, we use the MMHT14 parton distribution functions [25], with the associated values of α_s. We focus on two experimental data sets, which are sufficiently representative of the full body of data on low-mass Drell-Yan production: from the PHENIX experiment [26] at the BNL RHIC collider ($\sqrt{s}$ = 200 GeV) and from the NuSea (E866) fixed-target experiment [27, 28] at Fermilab ($\sqrt{s}$ = 38.8 GeV).

The main objective of our work will be to verify the perturbative convergence of the p_T distribution in low-mass Drell-Yan production, which is questionable [15] in view of NLO corrections being of comparable size to the LO predictions. In probing extreme kinematics where the application of perturbative QCD starts to become questionable, our results will also allow to better quantify and constrain the amount of non-perturbative contributions in these observables, thereby enabling the future usage of the relevant data-sets in quantitative model studies of non-perturbative effects.

2 Numerical results for Phenix

The PHENIX experiment is a multi-purpose detector at the BNL RHIC collider. It studies proton-proton and ion-ion collisions at various center-of-mass energies. For the measurement of low-mass lepton pair production [26], proton-proton collisions at a center-of-mass energy $\sqrt{s} = 200$ GeV were analysed. The measurement of the transverse momentum (p_T) distribution of the lepton pair in the range $p_T = 0$–6 GeV was performed in a single bin in the lepton pair invariant mass 4.8 GeV $< Q <$ 8.2 GeV, and restricting the lepton pair rapidity to the forward and backward regions $1.2 < |y| < 2.2$, which are summed. The data were corrected to full acceptance for fiducial selection cuts on the individual leptons.

We compute the p_T-distribution using NNLOJET using the vector-boson-plus-jet calculation with the jet requirement replaced by a minimum cut on p_T. Consequently, no fixed-order prediction is obtained for the leftmost bin, which includes $p_T = 0$ GeV as boundary. The fixed-order prediction for the p_T distribution diverges for low p_T, and should be supplemented by an all-order resummation of large logarithmic corrections.

The predictions for the p_T-distribution at LO, NLO and NNLO are displayed in Figure 1. We consider two choices for the central scale used in the evaluations: $\mu_F = \mu_R = Q$ (left) and $\mu_F = \mu_R = E_T$ (right), with $E_T = \sqrt{Q^2 + p_T^2}$. At values of $p_T > 1.5$ GeV, we observe that the NNLO corrections are positive throughout, and almost independent on p_T for both scale choices. The increase over NLO amounts to +25% for either of the two central scales.

The uncertainty on the theory predictions is estimated through an independent variation of μ_F and μ_R by a factor 2 around the central scale, excluding the two combinations where μ_F and μ_R are changed in opposite directions (seven-point variation). We observe that a near-uniform NNLO scale uncertainty of ±15% if either E_T or Q is chosen as central scale, and an overlap of the NLO and NNLO theory uncertainty bands. Given that the difference between the two choices of central scales is only marginal, E_T is chosen as default central scale for the remainder of this study. The scale dependence arises mainly from the variation of μ_R, as can be seen in Figure 2.

With E_T as default central scale, we observe from Figure 1 that the PHENIX data for

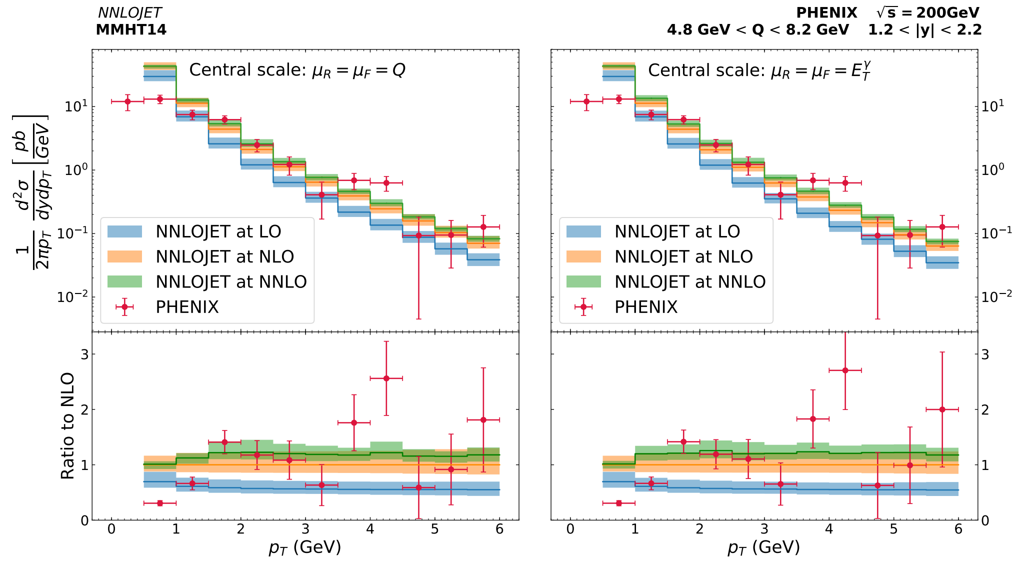

Figure 1: Transverse momentum distribution of lepton pairs, evaluated for central renormalization and factorization scales at Q (left) and E_T (right) and compared to data [26] from the PHENIX experiment.

$p_T > 1.5$ GeV are reasonably well-described within their respective uncertainties both at NLO and at NNLO. The inclusion of NNLO corrections leads to a better description of the normalization of the PHENIX data, which is however not significant in view of the large size of the experimental errors. Below $p_T = 1.5$ GeV, the fixed-order predictions exceed the data and fail to account for their shape indicating the onset of large logarithmic corrections that requires resummation. This observed transition into the resummation regime aligns well with a naive estimate based on the leading logarithmic behaviour compensating the suppression of the strong coupling, $C_F \frac{\alpha_s(Q)}{\pi} \ln^2(p_T^2/Q^2) \sim 1$.

3 Numerical results for NuSea

The NuSea experiment measured Drell-Yan lepton pair production on a fixed target at the Fermilab Tevatron with beam energy of 800 GeV, resulting in a centre-of-mass energy of $\sqrt{s} = 38.8$ GeV. Its initial objective was the determination of the flavour decomposition of the sea quark distributions in the proton through the measurement of cross section ratios between proton and deuterium targets [29]. Subsequent analysis of the large NuSea data set allowed measurements of absolute lepton pair production cross sections on protons [27, 28], multi-differential in the transverse momentum of the pair p_T, the invariant mass of the pair

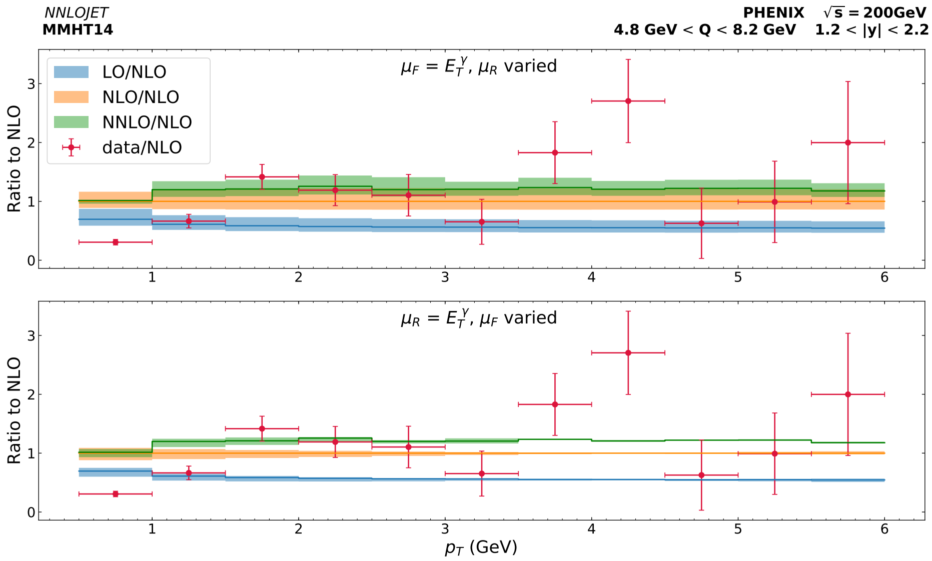

Figure 2: Dependence of transverse momentum distribution on variation of renormalization (upper frame) and factorization (lower frame) scales.

Q and Feynman-parameter $x_F = 2p_L/\sqrt{s}$, where p_L is the longitudinal momentum of the pair in the center-of-mass frame.

These measurements were made in six bins in Q, ranging between 4.2 GeV and 16.85 GeV, while excluding the Υ resonances. Each bin in Q was subdivided into four bins in x_F, between -0.05 in the backward direction and 0.8 in the very forward direction, where the p_T spectrum was then measured in a range up to 7 GeV at most. Owing to restrictions in the detector acceptance of NuSea, the maximal value of p_T is not attained for all combinations of Q and x_F, such that the p_T spectrum ends already at lower values in some of the bins. Moreover, especially for the larger values of Q and with x_F in the forward region, large values of p_T require parton momentum fractions (x_1, x_2) close to unity at Born-level. This is illustrated in Figure 3 for the mass bin 4.2 GeV$< Q < 5.2$ GeV; the higher mass bins correspond to even larger values of x_1 and x_2. In these regions, the fixed-order perturbative predictions vanish rapidly due to the decrease of the parton luminosity, while the experimental measurements may turn out to produce sizable cross sections even in these perturbatively disfavoured regions.

We compute the p_T-distributions for all (Q, x_F) bins where data are available, with NNLOJET using the vector-boson-plus-jet calculation with the jet requirement replaced by a minimum cut on p_T. The results are displayed in Figures 4–9. The fixed-order predictions of the p_T-distributions diverge for $p_T \to 0$, where an all-order resummation

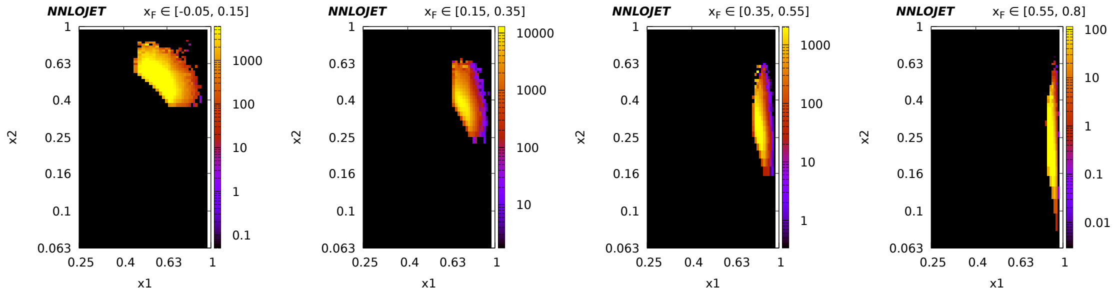

Figure 3: Range of parton momentum fractions x_1, x_2 that are resolved by the different x_F-bins in the NuSea measurement [27, 28], based on a leading-order computation for the mass range 4.2 GeV$< Q <$ 5.2 GeV. Color indicates the numerical magnitude of the contribution to the cross section.

of logarithmically enhanced terms is required for a meaningful prediction. Consequently, the left-most bin in p_T, which contains the $(p_T = 0)$-edge is discarded in our fixed-order computation. As for the PHENIX data considered in the previous section, we observe that for the NuSea kinematics, central scale choices of Q and E_T yield very similar central cross section values and uncertainty bands. We therefore make the choice of $\mu_F = \mu_R = E_T$ for the central scale, and theory uncertainties are estimated through a seven-point variation around the central scale values.

For several of the (Q, x_F) bins, we observe that the experimental data exceed the theory predictions by one order of magnitude or more. These cases typically correspond to kinematical situations that require one of the parton momentum fractions to be very close to unity. The large excess of experimental cross section measurements over theory expectations in these kinematical ranges may hint to large non-perturbative effects that distort the p_T spectra.

We observe that the NNLO QCD corrections are largely p_T-independent in all (Q, x_F) bins. They typically amount to an increase over the previously known NLO results which depend on the Q bin as follows: +35% for the lower two bins (Figures 4 and 5), +50% for the next two (Figures 6 and 7) and over +70% for the two bins of highest Q (Figures 8 and 9). A similar pattern is increasing corrections was already observed in going from LO to NLO. The increase at NNLO is within the NLO scale uncertainty bands for all Q bins. The scale uncertainties are reduced from NLO to NNLO, and are typically in a range around ±40%. The size of the NNLO corrections and the associated magnitude of the NNLO theory uncertainty is larger than in the case of PHENIX. This feature may be related to the lower centre-of-mass energy at NuSea, which consequently probes large parton momentum fractions, see Figure 3, where threshold logarithms are starting to influence the behaviour

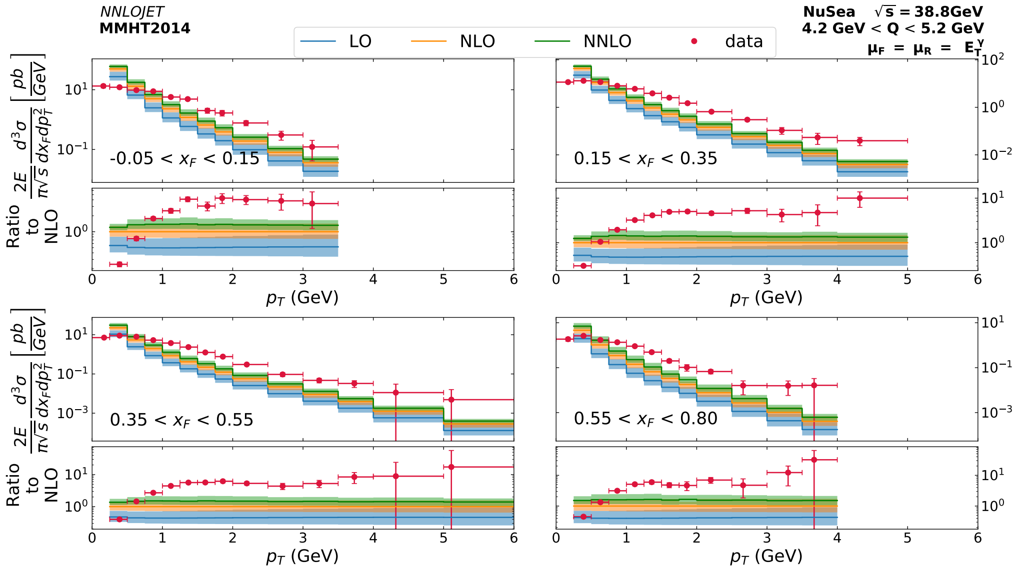

Figure 4: Transverse momentum distribution of lepton pairs with 4.2 GeV< Q < 5.2 GeV in different bins in x_F, compared to data from the NuSea experiment [27, 28].

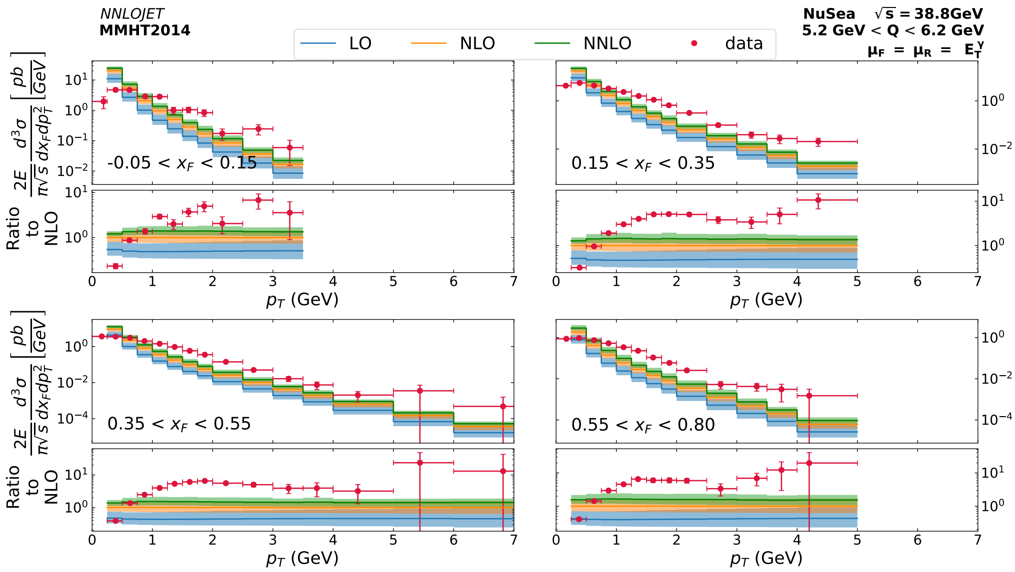

Figure 5: Transverse momentum distribution of lepton pairs with 5.2 GeV< Q < 6.2 GeV in different bins in x_F, compared to data from the NuSea experiment [27, 28].

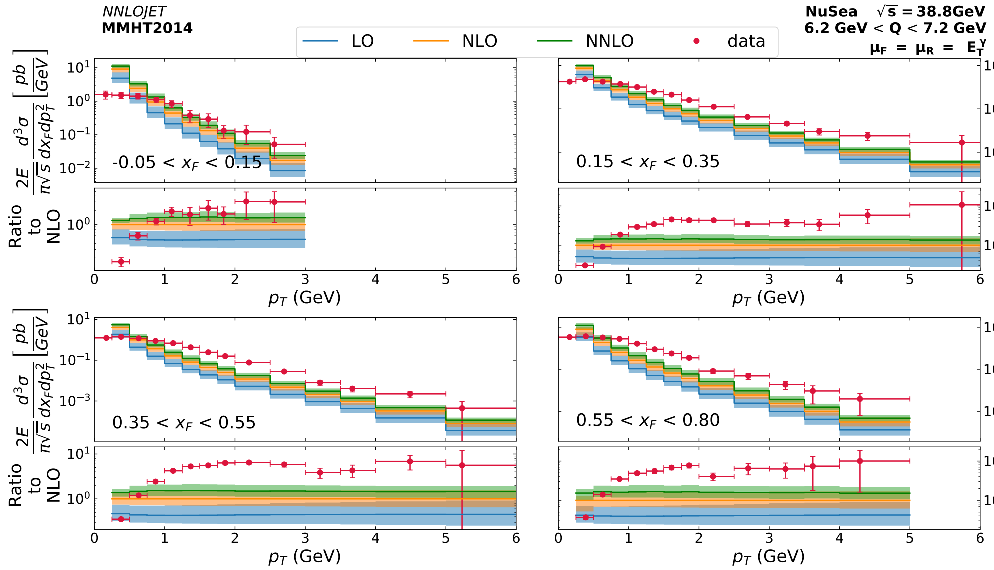

Figure 6: Transverse momentum distribution of lepton pairs with 6.2 GeV$< Q <$ 7.2 GeV in different bins in x_F, compared to data from the NuSea experiment [27, 28].

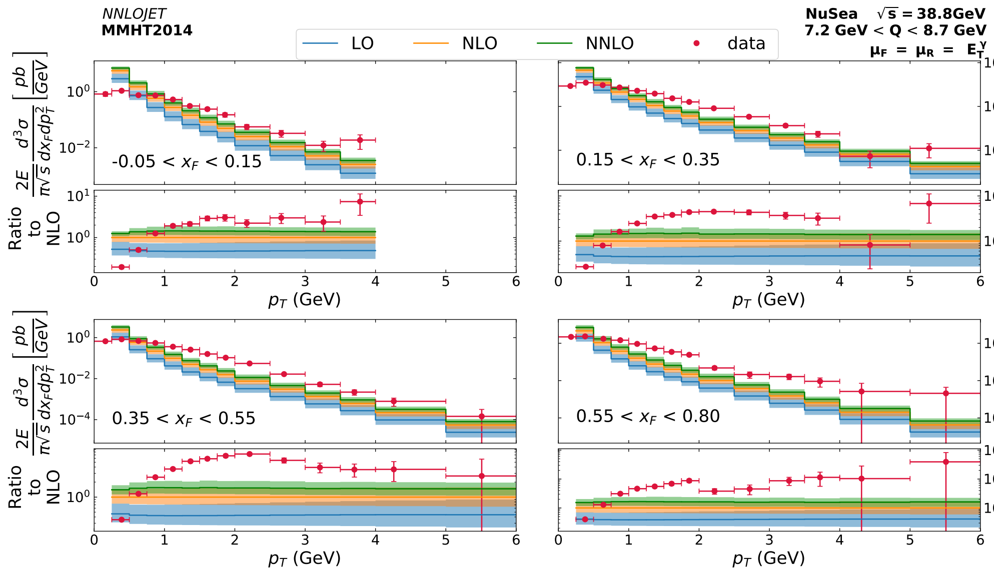

Figure 7: Transverse momentum distribution of lepton pairs with 7.2 GeV$< Q <$ 8.7 GeV in different bins in x_F, compared to data from the NuSea experiment [27, 28].

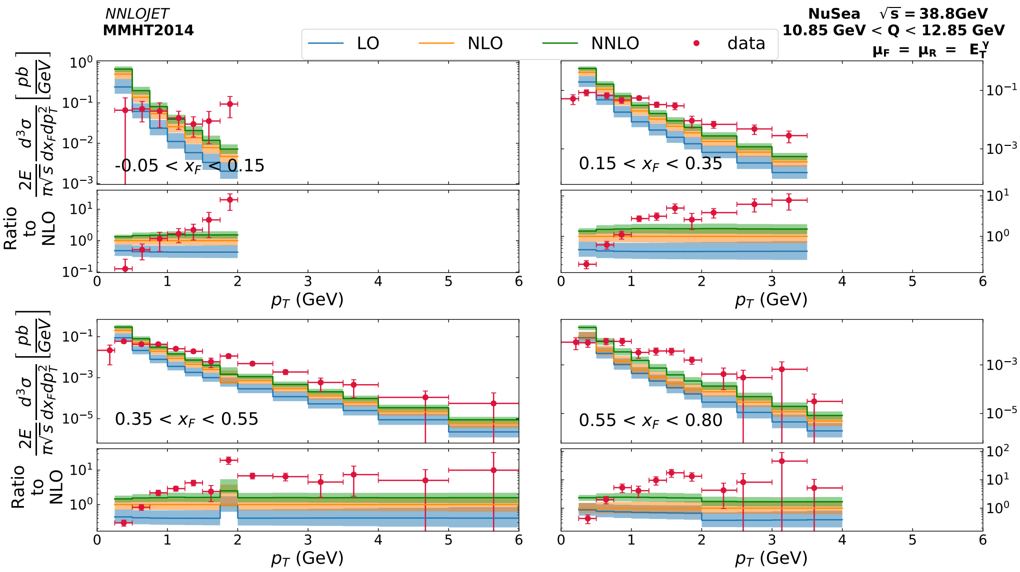

Figure 8: Transverse momentum distribution of lepton pairs with 10.85 GeV< Q < 12.85 GeV in different bins in x_F, compared to data from the NuSea experiment [27, 28].

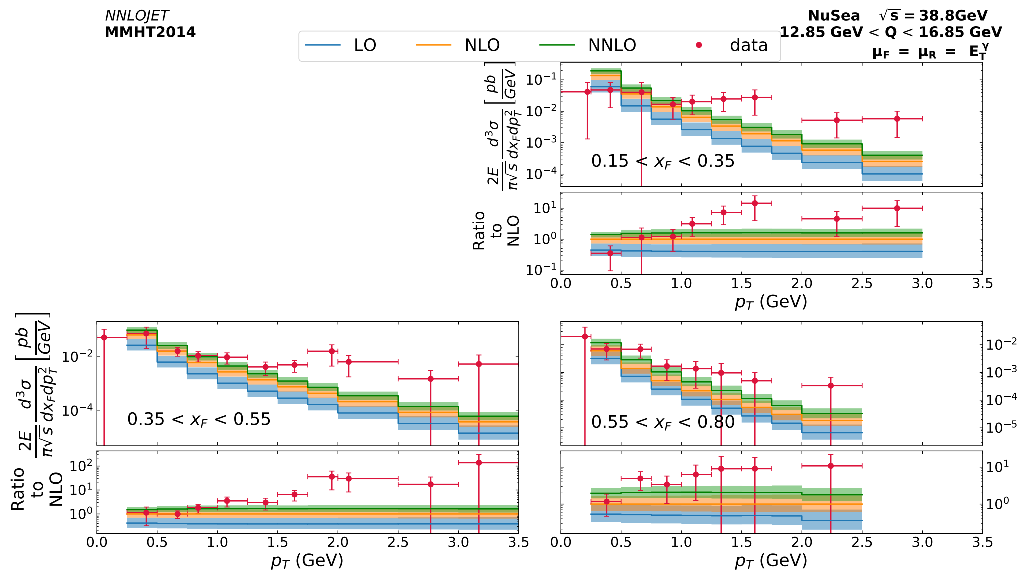

Figure 9: Transverse momentum distribution of lepton pairs with 12.85 GeV< Q < 16.85 GeV in different bins in x_F, compared to data from the NuSea experiment [27, 28].

of the perturbative higher-order coefficients starting from NLO onwards. The onset of threshold logarithms at $(x_1, x_2) \to 1$ also explains the increase of the corrections towards larger Q.

The newly computed NNLO corrections do not explain the large discrepancy between data and theory that was also previously observed at NLO level [15, 16]. In the majority of the (Q, x_F) bins, the ratio between data and NNLO theory approaches a constant value for $p_T \gtrsim 1$ GeV. The values of this ratio range between 1.5 for the central x_F bins and up to 10 for the forward x_F bins, with only a marginal dependence on the invariant mass Q. For $p_T < 1$ GeV, we do not expect the fixed order predictions to be meaningful due to their divergent behaviour at low p_T.

For increasing x_F, we observe that the p_T-distributions fall considerably more steeply towards larger values of p_T. This steeper decrease directly correlates with the larger data/theory ratios. It is very suggestive to observe that the p_T distributions in the vast majority of the (Q, x_F) bins could be brought in agreement with the data by shifting the value of p_T in the theory predictions by about $+1$ GeV when comparing to data. This observation could point to an intrinsic transverse momentum of the partons in the proton, which is caused by their non-perturbative bound-state dynamics.

Earlier studies have modelled this intrinsic transverse momentum effect in detail. In [16], it was shown that using transverse momentum dependent parton distributions (TMD) in combination with NLO fixed-order theory matched to parton-shower in the MC@NLO framework [17] leads to a satisfactory description of the NuSea data for the first bin in x_F and Q: $(-0.05 < x_F < 0.15$; 4.2 GeV$< Q < 5.2$ GeV$)$. This study could be repeated for the full range of (Q, x_F) in the light of the newly computed NNLO corrections.

The newly computed NNLO corrections are positive throughout all bins in x_F and Q, and largely p_T-independent. They indicate the need for a somewhat smaller shift of the p_T spectrum, as compared to NLO. This feature can be understood from the extra partonic recoil from one additional emission between NLO and NNLO, which does account for some (albeit small) part of the intrinsic transverse momentum. However, our results clearly show that perturbative emissions are insufficient to explain the p_T-spectrum at fixed target energies.

PDF uncertainties within the MMHT14 set were studied and found to be smaller than the residual scale uncertainties. It should however be emphasised that the behaviour of PDFs in the region relevant to the NuSea measurements is only poorly constrained by experimental data, such that their behaviour is largely determined by the extrapolation of the functional forms used in the PDF fitting procedure to large values of x. We have also re-computed the NNLO predictions for NuSea with the NNPDF3.1 parton distribution functions [30]. In contrast to MMHT14, the NNPDF3.1 quark and anti-quark distributions are negative at large values of x, which results in negative cross section predictions with the NNPDF3.1 set in several bins in x_F, especially for the larger Q values. Since the release of NNPDF3.1, positivity of parton distributions at large x has been revisited [31], it is now an inherent constraint in the new NNPDF4.0 release [32], while still remaining a matter of ongoing debate on formal grounds [33].

The NuSea data could provide important and unique constraints to the quark distributions in the proton at very large x, a region not covered by any other measurement. For them to be included in a global PDF determination will however require substantial advances in the understanding and quantitative modelling of non-perturbative effects that distort the p_T spectra in the NuSea kinematical range.

4 Conclusions

In this letter, we have investigated the impact of NNLO QCD corrections on the p_T-distribution of low-mass lepton pairs. This process is particularly interesting in view of probing the transition region between perturbative and non-perturbative dynamics in QCD. Previous studies [15, 16] based on NLO QCD have highlighted a poor perturbative convergence and displayed substantial discrepancies between theory predictions and experimental data. We focused our study on two representative data sets from PHENIX ($\sqrt{s} = 200$ GeV) and NuSea ($\sqrt{s} = 38.8$ GeV), which probe similar final-state kinematics at different collision energies, thereby probing different regions of parton momentum fractions. In either case, we observe large positive NNLO QCD corrections in the range of +25% in the case of the theoretical predictions to the PHENIX data and between +35% and +70% in the case of the theoretical predictions to the NuSea data, which are within the previously quoted NLO theory uncertainties, and which indicate the onset of perturbative convergence. The PHENIX data are described at NNLO QCD in a satisfactory manner. In contrast, the NNLO QCD prediction remains considerably below the NuSea data. This discrepancy increases with increasing x_F, which translates into larger values of parton momentum fractions being probed, which may indicate enhanced sensitivity to non-perturbative effects in these extreme kinematical regions.

Acknowledgments

This research is supported by the Dutch Organisation for Scientific Research (NWO) through the VENI grant 680-47-461, by the UK Science and Technology Facilities Council

(STFC) through grant ST/T001011/1, by the Swiss National Science Foundation (SNF) under contract 200021-197130 and by the Swiss National Supercomputing Centre (CSCS) under project ID ETH5f.

Furthermore we thank Xuan Chen, Juan Cruz-Martinez, James Currie, Marius Höfer, Matteo Marcoli, Jonathan Mo, Tom Morgan, Jan Niehues, Robin Schürmann, João Pires, Duncan Walker, and James Whitehead for useful discussions and their many contributions to the NNLOJET code.

References

[1] S. D. Drell and T.-M. Yan, *Massive Lepton Pair Production in Hadron-Hadron Collisions at High-Energies*, *Phys. Rev. Lett.* **25** (1970) 316–320. [Erratum: Phys.Rev.Lett. 25, 902 (1970)].

[2] K. Melnikov and F. Petriello, *Electroweak gauge boson production at hadron colliders through $O(\alpha_s^2)$*, *Phys. Rev. D* **74** (2006) 114017, [hep-ph/0609070].

[3] S. Catani, L. Cieri, G. Ferrera, D. de Florian, and M. Grazzini, *Vector boson production at hadron colliders: a fully exclusive QCD calculation at NNLO*, *Phys. Rev. Lett.* **103** (2009) 082001, [arXiv:0903.2120].

[4] C. Duhr, F. Dulat, and B. Mistlberger, *Drell-Yan Cross Section to Third Order in the Strong Coupling Constant*, *Phys. Rev. Lett.* **125** (2020) 172001, [arXiv:2001.07717].

[5] X. Chen, T. Gehrmann, N. Glover, A. Huss, T.-Z. Yang, and H. X. Zhu, *Dilepton Rapidity Distribution in Drell-Yan Production to Third Order in QCD*, *Phys. Rev. Lett.* **128** (2022) 052001, [arXiv:2107.09085].

[6] A. Gehrmann-De Ridder, T. Gehrmann, E. W. N. Glover, A. Huss, and T. A. Morgan, *Precise QCD predictions for the production of a Z boson in association with a hadronic jet*, *Phys. Rev. Lett.* **117** (2016) 022001, [arXiv:1507.02850].

[7] A. Gehrmann-De Ridder, T. Gehrmann, E. W. N. Glover, A. Huss, and T. A. Morgan, *The NNLO QCD corrections to Z boson production at large transverse momentum*, *JHEP* **07** (2016) 133, [arXiv:1605.04295].

[8] R. Boughezal, J. M. Campbell, R. K. Ellis, C. Focke, W. T. Giele, X. Liu, and F. Petriello, *Z-boson production in association with a jet at next-to-next-to-leading order in perturbative QCD*, *Phys. Rev. Lett.* **116** (2016) 152001, [arXiv:1512.01291].

[9] W. Bizoń, X. Chen, A. Gehrmann-De Ridder, T. Gehrmann, N. Glover, A. Huss, P. F. Monni, E. Re, L. Rottoli, and P. Torrielli, *Fiducial distributions in Higgs and Drell-Yan production at N^3LL+NNLO*, *JHEP* **12** (2018) 132, [arXiv:1805.05916].

[10] M. A. Ebert, J. K. L. Michel, I. W. Stewart, and F. J. Tackmann, *Drell-Yan q_T resummation of fiducial power corrections at N^3LL*, *JHEP* **04** (2021) 102, [arXiv:2006.11382].

[11] S. Alioli, C. W. Bauer, A. Broggio, A. Gavardi, S. Kallweit, M. A. Lim, R. Nagar, D. Napoletano, and L. Rottoli, *Matching NNLO predictions to parton showers using N3LL color-singlet transverse momentum resummation in geneva*, *Phys. Rev. D* **104** (2021) 094020, [arXiv:2102.08390].

[12] S. Camarda, L. Cieri, and G. Ferrera, *Drell–Yan lepton-pair production: qT resummation at N3LL accuracy and fiducial cross sections at N3LO*, *Phys. Rev. D* **104** (2021) L111503, [arXiv:2103.04974].

[13] W.-L. Ju and M. Schönherr, *The q_T and $\Delta\phi$ spectra in W and Z production at the LHC at N^3LL'+N^2LO*, *JHEP* **10** (2021) 088, [arXiv:2106.11260].

[14] Z.-B. Kang, J.-W. Qiu, and W. Vogelsang, *Low-mass lepton pair production at large transverse momentum*, *Phys. Rev. D* **79** (2009) 054007, [arXiv:0811.3662].

[15] A. Bacchetta, G. Bozzi, M. Lambertsen, F. Piacenza, J. Steiglechner, and W. Vogelsang, *Difficulties in the description of Drell-Yan processes at moderate invariant mass and high transverse momentum*, *Phys. Rev. D* **100** (2019) 014018, [arXiv:1901.06916].

[16] A. Bermudez Martinez et al., *The transverse momentum spectrum of low mass Drell–Yan production at next-to-leading order in the parton branching method*, *Eur. Phys. J. C* **80** (2020) 598, [arXiv:2001.06488].

[17] J. Alwall, R. Frederix, S. Frixione, V. Hirschi, F. Maltoni, O. Mattelaer, H. S. Shao, T. Stelzer, P. Torrielli, and M. Zaro, *The automated computation of tree-level and next-to-leading order differential cross sections, and their matching to parton shower simulations*, *JHEP* **07** (2014) 079, [arXiv:1405.0301].

[18] I. Scimemi and A. Vladimirov, *Non-perturbative structure of semi-inclusive deep-inelastic and Drell-Yan scattering at small transverse momentum*, *JHEP* **06** (2020) 137, [arXiv:1912.06532].

[19] V. Bertone, I. Scimemi, and A. Vladimirov, *Extraction of unpolarized quark transverse momentum dependent parton distributions from Drell-Yan/Z-boson production*, *JHEP* **06** (2019) 028, [arXiv:1902.08474].

[20] A. Bacchetta, V. Bertone, C. Bissolotti, G. Bozzi, F. Delcarro, F. Piacenza, and M. Radici, *Transverse-momentum-dependent parton distributions up to N^3LL from Drell-Yan data*, *JHEP* **07** (2020) 117, [arXiv:1912.07550].

[21] A. Vladimirov, *Pion-induced Drell-Yan processes within TMD factorization*, *JHEP* **10** (2019) 090, [arXiv:1907.10356].

[22] A. Gehrmann-De Ridder, T. Gehrmann, and E. W. N. Glover, *Antenna subtraction at NNLO*, *JHEP* **09** (2005) 056, [hep-ph/0505111].

[23] A. Daleo, T. Gehrmann, and D. Maitre, *Antenna subtraction with hadronic initial states*, *JHEP* **04** (2007) 016, [hep-ph/0612257].

[24] J. Currie, E. W. N. Glover, and S. Wells, *Infrared Structure at NNLO Using Antenna Subtraction*, *JHEP* **04** (2013) 066, [arXiv:1301.4693].

[25] L. A. Harland-Lang, A. D. Martin, P. Motylinski, and R. S. Thorne, *Parton distributions in the LHC era: MMHT 2014 PDFs*, *Eur. Phys. J. C* **75** (2015) 204, [arXiv:1412.3989].

[26] **PHENIX** Collaboration, C. Aidala et al., *Measurements of $\mu\mu$ pairs from open heavy flavor and Drell-Yan in $p+p$ collisions at $\sqrt{s} = 200$ GeV*, *Phys. Rev. D* **99** (2019) 072003, [arXiv:1805.02448].

[27] **NuSea** Collaboration, J. C. Webb et al., *Absolute Drell-Yan dimuon cross-sections in 800 GeV / c pp and pd collisions*, hep-ex/0302019.

[28] J. C. Webb, *Measurement of continuum dimuon production in 800-GeV/C proton nucleon collisions*. PhD thesis, New Mexico State U., 2003. hep-ex/0301031.

[29] **NuSea** Collaboration, E. A. Hawker et al., *Measurement of the light anti-quark flavor asymmetry in the nucleon sea*, *Phys. Rev. Lett.* **80** (1998) 3715–3718, [hep-ex/9803011].

[30] **NNPDF** Collaboration, R. D. Ball et al., *Parton distributions from high-precision collider data*, *Eur. Phys. J. C* **77** (2017) 663, [arXiv:1706.00428].

[31] A. Candido, S. Forte, and F. Hekhorn, *Can $\overline{\mathrm{MS}}$ parton distributions be negative?*, *JHEP* **11** (2020) 129, [arXiv:2006.07377].

[32] R. D. Ball et al., *The Path to Proton Structure at One-Percent Accuracy*, arXiv:2109.02653.

[33] J. Collins, T. C. Rogers, and N. Sato, *Positivity and renormalization of parton densities*, arXiv:2111.01170.